STRUCTURAL AND ELECTRONIC PROPERTIES OF $CsPbBr_3$ PEROVSKITE NANOCRYSTAL ON ZnO $(10\bar{1}0)$ NON-POLAR SURFACE

ABBAS Ghulam[1*], PYRCHLA Krzysztof[1], HAKIMI RAAD Naser[1], UKRAINTSEV Egor[1], REZEK Bohuslav[1]

[1]*Faculty of Electrical Engineering, Czech Technical University in Prague, Prague, Czechia, EU,*
*abbasghu@fel.cvut.cz

https://doi.org/10.37904/nanocon.2025.5180

Abstract

Oleic acid (OA) and oleylamine (OAm) ligands are commonly employed to enhance the stability of $CsPbBr_3$ (CPB) nanocrystals by passivation of the surface defects resulting in the improvement of photoluminescence efficiency, carrier lifetime and the adjustment of electronic properties. Studying the interaction between CPB perovskite and various ZnO surfaces is crucial for understanding the structural, electronic, and optical properties - such as bandgap, charge transport, and binding energy. Here we study the impact of OA and OAm ligands and non-polar ZnO surface $(10\bar{1}0)$) on the electronic properties of CPB. We perform structural and electronic analysis comparing DFT, DFT-1/2 and DFTB formalism to understand the contribution of each component towards the applications for scintillators and solar cells.

Keywords: Perovskite, ligands, Zinc Oxide (ZnO) surfaces, Density Functional Theory (DFT)

1. INTRODUCTION

Semiconductor $CsPbBr_3$ (CPB) perovskites have attracted significant attention due to their electronic, optical, superconductivity, magneto-resistive and thermodynamic properties. These I-IV-VII materials exhibit striking semiconducting properties like tunable bandgap which prominent them to be used in applications including photovoltaic[1], absorbers[2], solar cells[3], scintillators[4] and detectors[5]. CPB perovskites are characterized by general relation ABX_3, where A (Cs^+) represents a monovoltaics cation, B (Pb^{2+}) a divalent cation and X (Br^-) a halide anion.[5,6,7] Additionally, CPB contains multiple phases, cubic phase at high temperature, tetragonal phase as the temperature decreases and orthorhombic at room temperature. These phases influence the optoelectronic and structural properties of CPB.[8] Furthermore, surface properties of CPB perovskites are significant to study optoelectronic performance of these materials. The nonpolar CsBr-terminated surface shows the best stability, which is attributed to the effect of surface relaxation and high ionicity of the surface layer. The charge transfer to compensate the polarity, raises the energy of polar surfaces, which make polar surfaces unstable. Modulation of surface chemical composition can be applied to compensate polarity issues and lead towards stable CPB polar surfaces.[9] One of the notable property of CPB is its tunable direct bandgap which makes it highly suitable for green light emission, display technologies and photodetectors applications.[5]

Inorganic CPB shows better stability under ambient conditions than hybrid perovskites that often suffer from moisture-induced degradation. Still CPB is not entirely immune to ambient conditions and together with the toxicity of lead it hinders its applications. Understanding this degradation process is crucial to enhance the CPB durability in different applications.[10] Generally, different types of coating or ligands have been investigated to improve the stability of CPB.

Merging CPB with ZnO may offer additional route for stabilization and more efficient charge transfer. Zinc oxide (ZnO) is direct wide bandgap (3.3 eV) semiconductor renowned for its distinctive optical, structural, biomedical,

electrical and physical properties.[11] A wurtzite ZnO crystal exhibits four dominant crystallographic facets, (0001), $(000\bar{1})$, $(10\bar{1}0)$ and $(11\bar{2}0)$, each exhibiting distinct properties that influence the material behavior.[12] The (0001) Zn-faced and $(000\bar{1})$ O-faced are polar surfaces while $(10\bar{1}0)$ and $(11\bar{2}0)$ are non-polar surfaces.

Polarity arises from the asymmetrical distribution of the cations (Zn) and anions (O) in the lattice. The presence of a dipole moment across the unit cell leads to different chemical and physical properties on these surfaces.[13] The stability of polar surfaces has been a subject of interest, and several mechanisms and different possibilities are proposed to stabilize ZnO polar surfaces. Non-polar facets are characterized by alternating planes of Zn and O atoms, resulting in reduced surface dipoles. The non-polar facets contribute to their stability and influence the optoelectronic properties of ZnO nanostructures. Generally they offer higher values of binding energy and charge transfer resulting better adsorption of amino acids.[12] Comprehension of these distinct ZnO facets is fundamental for tailoring the material performance in various applications including catalysis, sensing and optoelectronic devices.

In this study, prior to integrating the complete system to study optoelectronic characteristics, all ZnO facets, CPB nanocrystal and oleic ligands are optimized individually to achieve their minimum energy level, ensuring stability in the final model. Following the assembly, an optimization process is conducted on the complete system. Subsequent calculations of structural and electronic properties including band structure and density of states (DOS) are performed.

2. METHODS

Density functional theory (DFT) is a first principal quantum mechanical method, based on atomic structure of materials it is used to calculate the electronic properties. DFT uses the Kohn-Sham equations while considering the electrons explicitly via the electron density.[12] It provides microscopic accuracy to understand interface and surface properties. We apply DFT based methods to understand the electronic properties of ZnO and CPB, individually and further when there is interface between ZnO and CPB. The Quantum ATK package is used to perform the structural and electronic properties calculations using DFT, DFT- ½ and density-functional tight-binding (DFTB). Specifically, this study has considered the atomic-level interaction of ZnO non-polar surface, namely the $(10\bar{1}0)$ facet with the CPB (100) nanocrystal. At first, the interaction between CPB cube and ligands is studied to understand the impact of ligands on electronic properties of CPB. In the second step, to assess the influence of ZnO facets on optoelectronic properties of the system, a CPB cube with fixed orientation (100) is added to non-polar slab of ZnO. Both CPB and ZnO structures are optimized using the Linear Combination of Atomic Orbitals (LCAO) calculator with GGA-PBE exchange-correlation functional implemented in DFT formalism. To confirm the numerical accuracy, density mesh cutoff of 125 Hartree and Monkhorst-Pack scheme with a 3×3×1 k-point grid is applied. The atomic coordinates are relaxed using a conjugate gradient method until all forces are below 0.01 eV/Å.

Subsequently, the oleic ligands, specifically oleic acid (OA) and oleylamine acid (OAm), are oriented perpendicular to the CPB cube to investigate the ligand-surface interactions. To avoid nonphysical interactions arising from periodic boundary conditions, a vacuum greater than 20 Å is considered along Z-axis. Further, proper periodic boundary conditions are employed in the X and Y directions, while Neumann and Dirichlet boundary conditions are used along the left and right of C direction, respectively, to accurately model the system's physical constraints. In the present study, the electronic properties of cubic CPB structure containing 135 atoms are investigated from atomic and electronic level using DFT and DFT- ½ methods. The cubic phase is selected due to its prototype structure of perovskites and wider applications at the nano level. For ZnO calculations, DFT, DFT- ½ and density-functional tight-binding (DFTB) simulations are used and the results are compared with bulk ZnO band gap of 3.44 eV at low temperatures and 3.37 eV at room temperature, respectively.[14] Finally, DFT and DFT- ½ are used to study the heterostructure containing ZnO and CPB.

3. RESULTS AND DISCUSSION

3.1 Electronic properties of cubic $CsPbBr_3$ (100)

The CPB structure containing 135 atoms (**Figure 1(a)**) was optimized to its minimum energy level to calculate the electronic properties. The band structure of optimized CPB (100) surface (**Figure 1(b)**) exhibits semiconducting behavior with a bandgap of approximately-2.22 eV. The bandgap value is confirmed by density of states profile shown also in **Figure 1(b)**. The fundamental band gap of the cubic CPB structure is slightly less than the bulk CPB value (~2.3 eV). Using DFT-1/2 the bandgap 3.63 eV was calculated, as shown in **Table 1**. But as discussed in Ref.[5], the bandgap can be modified by changing the surface thickness. Our results reveal the significance of the applied method as well. The presence of Fermi level (E_F) at the middle of the bandgap indicates its intrinsic behavior with the direct bandgap. Our results of electronic bandgap calculated from DFT are consistent with the previous results obtained using different higher order DFT functionals.

To study the band structure and density of states, DFT ½ method was also considered. As shown in **Table 1** the value of bandgap 3.63 eV is calculated. This value of bandgap is more than the experimental range 1.23-3.10 eV [5], but it is tunable by the crystal thickness. The results in **Figure 1 (b)** reveal that CPB (100) nanocrystal preserves the semiconducting behavior. The band structure and density of states analysis show absence of mid-gap states. It shows that the surface dangling bonds do not direct to severe mid-gap trap states consistent with high photoluminescence quantum yields and bright emission of CPB nanocrystals commonly observed in experiments.

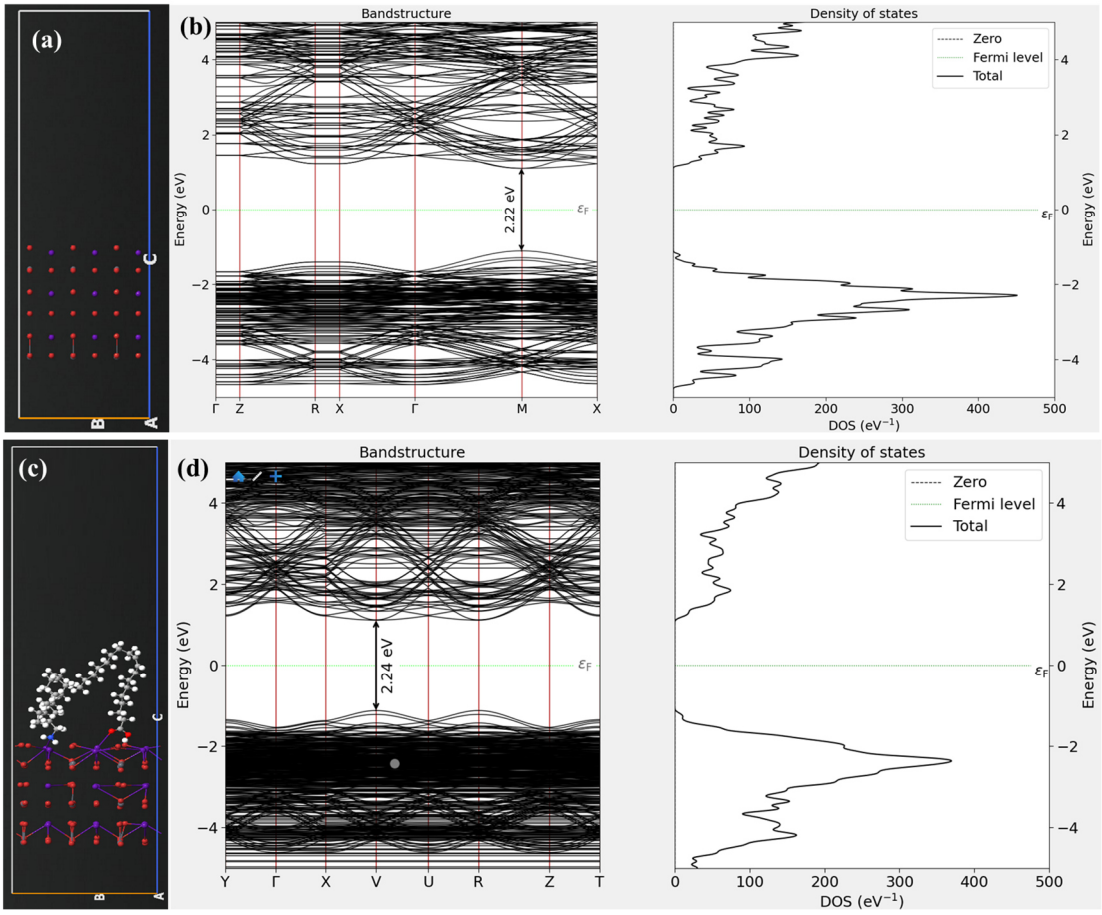

Figure 1 (a) optimized atomistic model, (b) band structure and DOS analysis of CPB structure. (c) optimized atomistic model, (d) band structure and DOS analysis of CPB with oleic ligands (OA/OAm). All calculated using DFT simulations.

The interaction of surface ligands like OA and OAm with CPB can modulate different properties of CPB including electronic coupling, binding energy and adsorption. **Figure 1 (c)** shows the optimized structure where OA and OAm ligands have been attached to CPB surface. The optimized structure in **Figure 1(c)** reveals covalent bond with bond length 3.16 Å among the Nitrogen atom and Cesium atom in the case of ligand. When ligand interacts with CPB, its oxygen atom interacts with Cesium atom of CPB with bond length 3.17 Å. **Figure 1(d)** shows that the optimized CPB (100) surface with OA and OAm ligands exhibits semiconducting behavior, with the bandgap values of 2.24 eV using DFT and 2.65 by using DFT-1/2 as shown in the **Table 1**. The position of Fermi level (E_F) in the middle of the bandgap indicates intrinsic CPB behavior with the direct bandgap. Our findings show a small increase in the bandgap of CPB when ligands are introduced revealing that the presence of ligands does not significantly influence the band structure of CPB.[15] Furthermore, this attachment of ligands with CPB results in interfacial charge interaction which introduces the localization of electron distribution inside the ligand molecules. To understand this charge transfer, Mulliken charge distribution analysis was performed. The net charge was calculated as:

$$Q_{net} = Q_{after\ adsorption} - Q_{before\ adsorption} \qquad (1)$$

Our Mulliken charge calculations analysis reveals a net charge transfer of −0.118 e from the OA and OAm ligands to the CPB (100) surface, indicating ligand-to-surface electron transfer. This shows the donor nature of OA and OAm ligands, as they interact with surface Cs atoms. This charge transfer plays important role in stabilization of CPB and in modulation of its electronic structure, which is crucial from the perspective of scintillator applications. Electron donated from OA and OAm ligands can effectively passivate the surface defect states particularly associated with halide vacancies resulting in enhancing radiative recombination efficiency and can improve energy resolution and scintillation light yield. As a result, at the interface an electron-rich reaction microenvironment is generated by localized interfacial electrons, at the boundary energetic barriers and electronic states are reduced and the efficiency of interparticle energy transport to charge separation interfaces is enhanced. Consequently, it improves overall performance of CPB for photocatalytic applications.[10]

Table 1 The energetic band gap of CPB (100) nanocrystal with and without ligands calculated using DFT and DFT-1/2 methods.

	DFT (Band gap, eV)	DFT-1/2 (Band gap, eV)
CPB (100)	2.22	3.63
CPB (100) with ligands	2.24	2.65

3.2 Electronic properties of ZnO Surfaces

As shown in **Figure 2**, structural and electronic properties including optimization, band structure and DOS of ZnO facets (0001), $(000\bar{1})$, $(10\bar{1}0)$ and $(11\bar{2}0)$, respectively are calculated by employing DFTB.

Based on the Slater-Koster model a self-consistent tight-binding model using the znorg 0-1 parameter set, which has been built for simulations on Zn bulk, ZnO bulk, ZnO surfaces and ZnO interactions with organic molecules, was implemented.[16] The obtained bandgap values were 2.88 eV, 2.92 eV, 3.32 eV and 4.06 eV for ZnO (0001), $(000\bar{1})$, $(10\bar{1}0)$ and $(11\bar{2}0)$, respectively. As compared to bulk ZnO band gap of 3.37 eV, the band gap of $(11\bar{2}0)$ is higher probably because of well-known electron confinement phenomenon that occurs in the finite slabs. However, for ZnO polar facets (0001) and $(000\bar{1})$ the band gaps are lower than the bulk gap of ZnO, the possible reason might be the imposed vacancies on these ZnO surfaces for the stabilization purposes.[12] These results reveal that for given conditions the maximum valance band and minimum conduction band are sited at the Γ symmetry point of the Brillouin zone. DOS analysis shows that the valance band maximum (VBM) and conduction band minimum (CBM) at the Γ point and the surronding parts, originating from 4s states of Zn and 2p states of O atoms respectively.

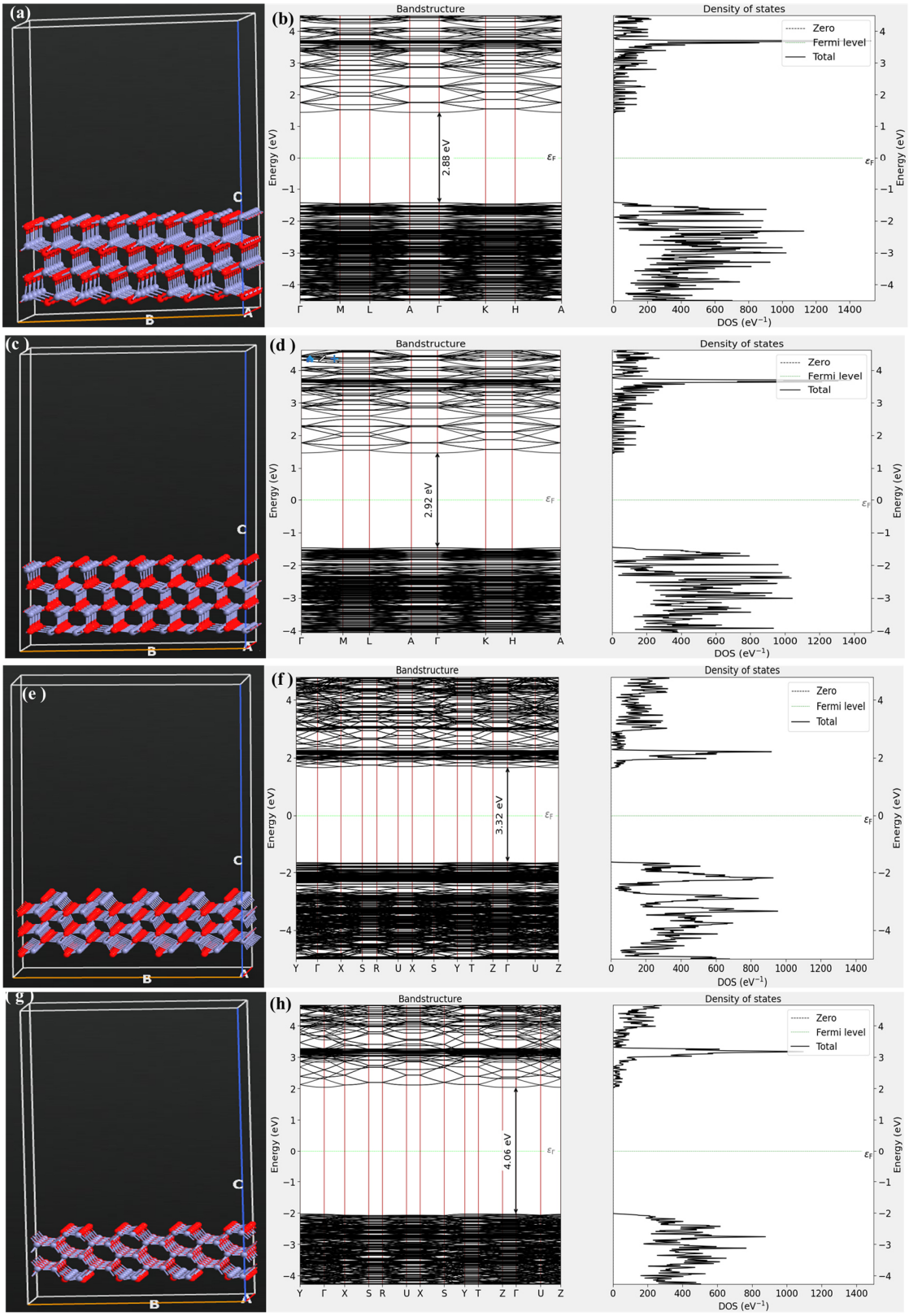

Figure 2 (a) Atomistic model, (b) band structure and DOS analysis of optimized Zn-face (0001), (c) Atomistic model, (d) band structure and DOS analysis of optimized O-face $(000\bar{1})$, (e) Atomistic model, (f) band structure and DOS analysis of optimized non-polar $(10\bar{1}0)$, (g) Atomistic model, (h) band structure and DOS analysis of optimized non-polar $(11\bar{2}0)$ ZnO facets.

Table 2 The energetic band gap of polar and non-polar ZnO facets calculated using DFT, DFT-1/2 and DFTB methods.

ZnO	DFT (Band gap, eV)	DFT-1/2 (Band gap, eV)	DFTB (Band gap, eV)
0001	0.625	2.305	2.876
$000\bar{1}$	0.515	2.026	2.924
$10\bar{1}0$	0.377	1.336	3.320
$11\bar{2}0$	1.600	3.140	4.070

3.3 Electronic properties of $CsPbBr_3$ cube interacting with nonpolar ZnO $(10\bar{1}0)$ surface

Figure 3 summarizes the results of simulations for ZnO non-polar facet $(10\bar{1}0)$) and CPB (100) cubic structure in one system. **Figure 3(a)** presents the optimized structure of CPB (100) over ZnO non-polar facet $(10\bar{1}0)$. The simulations indicate bonding between Zn and Br atoms and O with Pb atoms. The Zn atoms contain positive charge while oxygen atoms have negative charges. In $CsPbBr_3$, Cs and Pb are positive while Br_3 is negative. When ZnO interacts with $CSpbBr_3$ (CPB), the rearrangement will occur with average distance of 2.59 Å between Zn atoms and Br atoms. The band structure and DOS analysis in **Figure 3(b)** reveals different electronic structure compared to CPB and ZnO components alone. Band gap is now only 1.19 eV. The smaller value of energy gap between HOMO and LUMO means higher value of charge transfer between CPB and ZnO parts.

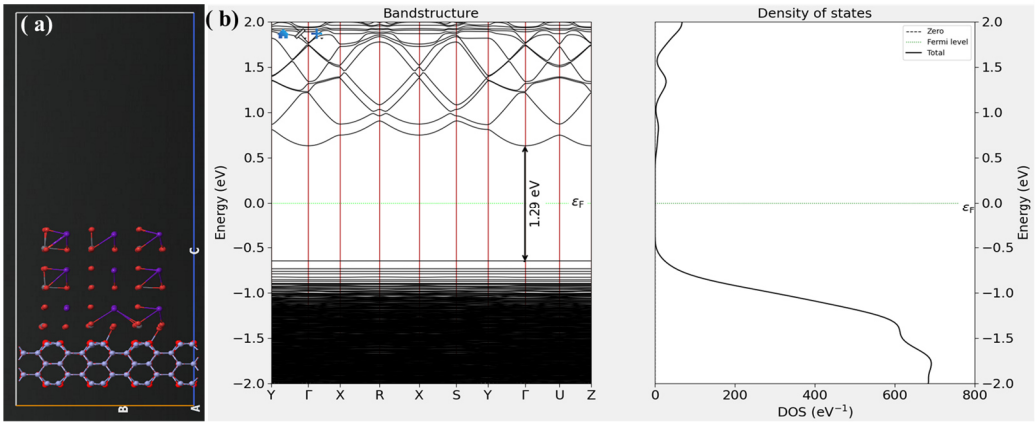

Figure 3 (a) Atomistic model, (b) band structure and DOS analysis of optimized non-polar $(10\bar{1}0)$ ZnO facets.

4. CONCLUSION

Structural, electrical and optical properties of non-polar CPB cubic structure were analyzed. The band structure, DOS and optical properties were studied by using DFT and DFT-1/2. The impact of ligands and non-polar ZnO surfaces on the CPB electronic properties was also analyzed. We conclude that the band structure of CPB can be tuned to by interacting with ligands or nonpolar ZnO surface $(10\bar{1}0)$ which can facilitate lower band gap energy and charge transfer. Both features can be beneficial for energy harvesting applications and scintillators.

ACKNOWLEDGEMENTS

This research was supported by the Grant Agency of the Czech Republic project 24-12872S and by the Ministry of Education Youth and Sports project CZ.02.01.01/00/22_008/0004617 (EcoStor) under the Operational Program Johannes Amos Comenius, call Excellent Research.

REFERENCES

[1] LIU, Y.; ZHANG, L.; WANG, M.; ZHONG, Y.; HUANG, M.; LONG, Y.; ZHU, H. Bandgap-tunable double-perovskite thin films by solution processing. *Materials Today*. 2019, vol. 28, pp. 25–30.

[2] QI, F.; FU, X.; MENG, L.; LU, C.-Z. Exploring high-performance all-inorganic perovskite materials for next-generation photovoltaic applications: a theoretical study on cs2tlbix6 (x = cl, br, i). *Computational and Theoretical Chemistry*. 2024, vol. 1233, pp. 114500.

[3] LEI, Y.; LI, Y.; LU, C.; YAN, Q.; WU, Y.; BABBE, F.; GONG, H.; ZHANG, S.; ZHOU, J.; WANG, R.; ZHANG, R.; CHEN, Y.; TSAI, H.; GU, Y.; HU, H.; LO, Y.-H.; NIE, W.; LEE, T.; LUO, J.; YANG, K.; JANG, K.-I.; XU, S. Perovskite superlattices with efficient carrier dynamics. *Nature*. 2022, vol. 608, no. 7922, pp. 317–323.

[4] CHEN, Q.; WU, J.; OU, X.; HUANG, B.; ALMUTLAQ, J.; ZHUMEKENOV, A. A.; GUAN, X.; HAN, S.; LIANG, L.; YI, Z.; LI, J.; XIE, X.; WANG, Y.; LI, Y.; FAN, D.; TEH, D. B. L.; ALL, A. H.; MOHAMMED, O. F.; BAKR, O. M.; WU, T.; BETTINELLI, M.; YANG, H.; HUANG, W.; LIU, X. All-inorganic perovskite nanocrystal scintillators. *Nature*. 2018, vol. 561, no. 7721, pp. 88–93.

[5] EZZELDIEN, M.; AL-QAISI, S.; ALROWAILI, Z. A.; ALZAID, M.; MASKAR, E.; ES-SMAIRI, A.; VU, T. V.; RAI, D. P. Electronic and optical properties of bulk and surface of cspbbr3 inorganic halide perovskite a first principles DFT 1/2 approach. *Scientific Reports*. 2021, vol. 11, no. 1, pp. 20622.

[6] MISHRA, K. K.; SHARMA, R. A. Comparative study of the structural, electronic, and optical properties of ca3sbcl3 halide perovskite using DFT-GGA and HSE06 functional for photovoltaic applications. *Optical and Quantum Electronics*. 2024, vol. 57, no. 1, pp. 44.

[7] LANG, L.; YANG, J.-H.; LIU, H.-R.; XIANG, H. J.; GONG, X. G. First-principles study on the electronic and optical properties of cubic abx3 halide perovskites. *Physics Letters A*. 2014, vol. 378, no. 3, pp. 290–293.

[8] XIE, S.; YANG, D.; LI, Z.; MA, X.; WANG, H.; LIU, S.; LIU, Y.; YUE, S. The evolution of electrical, optical, and mechanical properties of cspbbr3 perovskites during continuous phase transitions. *Chemical Engineering Journal*. 2025, vol. 505, pp. 159524.

[9] YANG, Y.; HOU, C.; LIANG, T.-X. Energetic and electronic properties of cspbbr3 surfaces: a first-principles study. *Physical Chemistry Chemical Physics*. 2021, vol. 23, no. 12, pp. 7145–7152.

[10] ZHONG, F.; SHENG, J.; DU, C.; HE, Y.; SUN, Y.; DONG, F. Ligand-mediated exciton dissociation and interparticle energy transfer on cspbbr3 perovskite quantum dots for efficient co2-to-co photoreduction. *Science Bulletin*. 2024, vol. 69, no. 7, pp. 901–912.

[11] HAN, Y.; GUO, J.; LUO, Q.; MA, C.-Q. Solution-processable zinc oxide for printed photovoltaics: progress, challenges, and prospect. *Advanced Energy and Sustainability Research*. 2023, vol. 4, no. 10.

[12] HEMATIAN, H.; UKRAINTSEV, E.; REZEK, B. Strong structural and electronic binding of bovine serum albumin to ZnO via specific amino acid residues and zinc atoms. *ChemPhysChem*. 2022, vol. 23, no. 2, pp. e202100639.

[13] Woll, C. The chemistry and physics of zinc oxide surfaces. *Progress in Surface Science*. 2007, vol. 82, no. 2–3, pp. 55–120.

[14] MANG, A.; REIMANN, K.; RÜBENACKE, ST. Band gaps, crystal-field splitting, spin-orbit coupling, and exciton binding energies in ZnO under hydrostatic pressure. *Solid State Communications*. 1995, vol. 94, no. 4, pp. 251–254.

[15] CHEN, J.; LIU, X.; XI, S.; ZHANG, T.; LIU, Z.; CHEN, J.; SHEN, L.; KAWI, S.; WANG, L. Functionalized Ag with thiol ligand to promote effective Co2 electroreduction. *ACS Nano*. 2022, vol. 16, no. 9, pp. 13982–13991.

[16] MOREIRA, N. H.; DOLGONOS, G.; ARADI, B.; DA ROSA, A. L.; FRAUENHEIM, T. Toward an accurate density-functional tight-binding description of zinc-containing compounds. *Journal of Chemical Theory and Computation*. 2009, vol. 5, no. 3, pp. 605–614.